

## Article

# Suggestions and Applications for Evaluating Seismic Functionality for Railway Infrastructure Network Based on Fragility Curve

Mintaek Yoo <sup>1</sup>, Jiyun Jeon <sup>1</sup>, Seokjung Kim <sup>2,\*</sup> and Sunnie Haam <sup>3,\*</sup>

<sup>1</sup> Department of Civil and Environmental Engineering, Gachon University, 1342 Seongnam-daero, Sujeong-gu, Seongnam-si 13120, Republic of Korea; mintakyoo@gachon.ac.kr (M.Y.); jiyunjeon@gachon.ac.kr (J.J.)

<sup>2</sup> Department of Geotechnical Division, Korea Institute of Civil Engineering and Building Technology (KICT), 283 Goyang-dearo, Ilsan-seogu, Goyang-si 10223, Republic of Korea

<sup>3</sup> Department of Fire Safety Engineering and Disaster Management, University of Seoul, 163 Seoulsiripdae-ro, Dongdaemun-gu, Seoul 02504, Republic of Korea

\* Correspondence: seokjungkim@kict.re.kr (S.K.); dandyhaam@uos.ac.kr (S.H.)

**Abstract:** This study proposes a novel model to quantitatively evaluate functionality loss in railway network systems during earthquakes and assesses its applicability to a hypothetical railway network system. The model combines seismic fragility functions and restoration curves to assess functionality loss, deriving a time-dependent recovery function to propose a functionality loss model based on earthquake magnitude. The proposed model uses a hypothetical railway network to calculate the overall functionality loss of the network under various earthquake scenarios. The hypothetical railway network was designed with three lines, allowing different routes to remain operational depending on the damaged sections and increasing the diversity of network impact scenarios based on the functionality loss. This model provides a framework for analyzing the functionality loss and recovery processes of railway networks during seismic events and assessing the socioeconomic impacts of earthquakes.

**Keywords:** seismic functionality; railway; infrastructure; network; fragility curve



Academic Editor: Tiago Filipe da Silva Miranda

Received: 4 December 2024

Revised: 3 January 2025

Accepted: 6 January 2025

Published: 8 January 2025

**Citation:** Yoo, M.; Jeon, J.; Kim, S.; Haam, S. Suggestions and Applications for Evaluating Seismic Functionality for Railway Infrastructure Network Based on Fragility Curve. *Appl. Sci.* **2025**, *15*, 534. <https://doi.org/10.3390/app15020534>

**Copyright:** © 2025 by the authors. Licensee MDPI, Basel, Switzerland. This article is an open access article distributed under the terms and conditions of the Creative Commons Attribution (CC BY) license (<https://creativecommons.org/licenses/by/4.0/>).

## 1. Introduction

Korea experienced the 2016 Gyeongju earthquake (magnitude 5.8) and the 2017 Pohang earthquake (magnitude 5.3). Globally, major earthquakes such as the 2019 Alaska earthquake (magnitude 7.0), the 2021 Haiti earthquake (magnitude 7.2), and the Turkey–Syria earthquake (magnitude 7.8) were observed. The Turkey–Syria earthquake included aftershocks ranging from magnitude 6.0 to 7.0, with the largest main earthquake reaching magnitude of approximately 7.5, indicating intense seismic activity. Such large-scale earthquakes and aftershocks have heightened anxiety about earthquakes and increased the need for preparedness and pre-disaster damage assessments. The recent increase in the construction of various railway facilities, such as the GTX and Shinansan lines, has expanded railway networks, increasing the need for studies on the seismic behavior of individual railway components [1]. Based on such seismic behavior evaluations, seismic fragility curves—which represent the exceedance probability of various damage states caused by earthquakes—have been proposed by several researchers and are widely used as quantitative indicators of structural damage [2–4].

When railway networks are damaged by earthquakes, the physical structures suffer direct damage, and socioeconomic losses such as disruptions of logistics due to the func-

tionality degradation of network components occur. Studies on structural behavior during earthquakes and seismic fragility functions have been conducted by numerous researchers. Nguyen et al. [5] studied the dynamic behavior of pile structures, while Yoo et al. [6] investigated the dynamic behavior of underground structures during earthquakes and proposed methods for risk assessment. Additionally, various studies on seismic fragility have been conducted. Kim et al. [7] developed seismic fragility functions for railway structures, presenting methods for evaluating seismic damage and developing fragility functions for tracks, bridges, and tunnels. Lee [8] assessed seismic performance and developed fragility functions for tunnels on the Gyeongbu high-speed railway line, comparing them with those of other studies. Yang and Kwak [9] analyzed the 2004 Niigata earthquake and developed seismic fragility curves for high-speed rail systems, concluding that long-period seismic waves significantly damage tunnels and bridges. Argyroudis and Pitilakis [2] developed seismic fragility curves for shallow tunnels to evaluate their vulnerability based on ground conditions, while Avanaki et al. [10] proposed fragility curves for steel fiber reinforced concrete segment tunnel linings, analyzing the impact of reinforcement materials on seismic performance. Andreotti and Lai [11] used seismic fragility curves for mountain tunnels to study methods for assessing tunnel vulnerability in seismic risk analyses. However, prior research on seismic fragility curves has primarily focused on the physical damage sustained by structures during earthquakes; limited studies quantitatively evaluated the socioeconomic impact, such as logistics disruptions, based on functionality loss of network components. Hu et al. [12] evaluated the impact of buried depth on the seismic fragility of tunnels embedded in soft soil. Kim et al. [13] investigated fragility functions for various railway structures and proposed and applied a direct damage propagation model; however, the study only analyzed direct damage and did not evaluate the functionality loss of structures. Zhongkai et al. [14] proposed a procedure to evaluate the recovery performance of tunnel structures; however, their study focused on analyzing the recovery performance of individual tunnel structures without examining the functionality loss at the network level.

In this study, we established a new railway network system and proposed a model to evaluate functionality loss during earthquakes by leveraging statistical data on existing seismic fragility curves and recovery times for bridges, embankments, and tunnels. The proposed model was defined using functionality loss curves for railway network components and enables the quantitative evaluation of the functionality loss based on earthquake magnitude. The proposed model was applied to the new railway network system to estimate the functionality loss to actual railway facilities during extreme seismic events. Based on the results of this study, the functionality loss of railway networks caused by earthquakes can be quantified, enabling the assessment of socioeconomic impacts such as logistics disruptions.

## 2. Derivation of Functionality Loss Evaluation Model for Railway Network Components

### 2.1. Procedure for Deriving Functionality Loss Evaluation Models for Railway Network Components

Railway networks consist of structures on which tracks are constructed, which can be broadly classified into tunnels, bridges, and embankments. Each component exhibits different functionality loss characteristics depending on the earthquake. The functionality loss model for each railway network component during earthquakes can be determined through the following process. First, the probability of various damage states during earthquakes of varying magnitudes must be calculated to evaluate the functionality loss caused by earthquakes. The damage to each structure caused by earthquakes is determined by the characteristics of the structure and can be defined using seismic fragility curves. Seismic fragility curves are integrated with the results of probabilistic seismic hazard analysis

(PSHA) and are used for seismic probabilistic risk assessment (SPRA) of target structures, showing the exceedance probabilities of each damage state based on the magnitude of the input earthquake [15]. Next, restoration curves are derived following the damage. Restoration curves can be constructed using the mean and standard deviation of recovery times for each damage state of the structure. By combining the derived seismic fragility and restoration curves, functionality curves can be obtained for each earthquake scenario over time. Functionality curves are derived as expected values by combining the probability of damage occurrence for each damage state and the degree of functionality degradation over time when the damage occurs, representing the predicted functionality recovery of the structure over time. Finally, the evaluation time for functionality loss is determined, and the area under the functionality degradation curve over time is calculated to derive the final functionality loss curve. The procedure, organized in sequential order, is as follows and the flowchart is described in Figure 1.

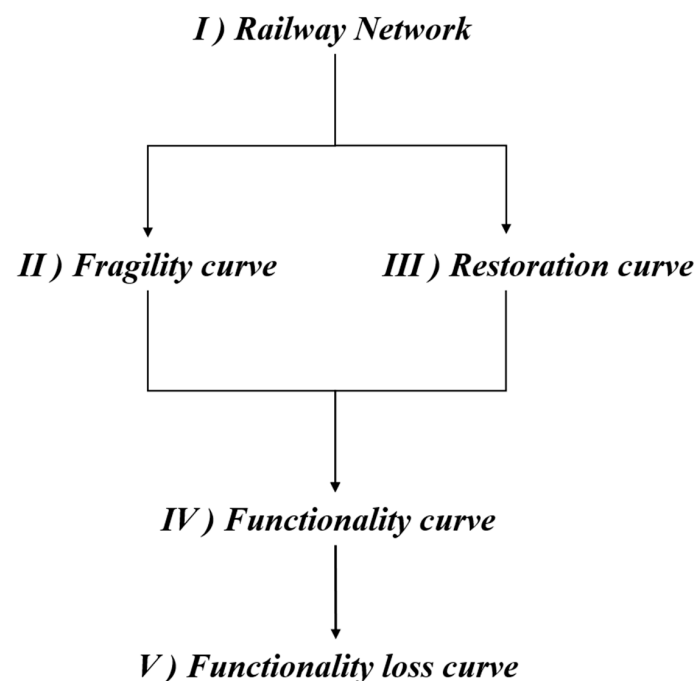


**Figure 1.** Procedure for development functionality loss curve evaluation.

1. Classification of railway network components
2. Determination of seismic fragility functions for each component (determination of probability functions for each damage state)
3. Determination of restoration curves for each component
4. Combination of seismic fragility functions and restoration curves to derive functionality functions based on earthquake intensity
5. Evaluation of functionality degradation over time to derive functionality loss functions based on earthquake intensity

## 2.2. Establishment of Functionality Loss Evaluation Models for Railway Network Components

### 2.2.1. Seismic Fragility Curves for Railway Network Components

We applied previously researched fragility curves for railway network components—bridges, tunnels, and embankments. For Korean railway bridges, PSC box girder bridges are predominant, and Kim et al. [13] proposed fragility curves for railway PSC box girder bridges by linearly combining three prior models. In this study, the proposed seismic fragility curves were applied to evaluate the seismic resilience of bridge components in the

railway network. The fragility curves are shown in Table 1 and Figure 2. The formula for deriving the seismic fragility function is presented in Equation (1).

$$P[ds|IM] = \Phi\left(\frac{\ln X - \mu}{\beta}\right) \tag{1}$$

where  $X$  represents the Peak Ground Acceleration,  $\mu$  denotes the median (g), and  $\beta$  represents the standard deviation (g).

**Table 1.** Fragility curve for railway bridge [13].

Damage State	Median (g)	Standard Deviation ( $\beta$ )
Slight	0.293	0.632
Moderate	0.464	0.677
Extensive	0.596	0.699
Complete	0.853	0.691

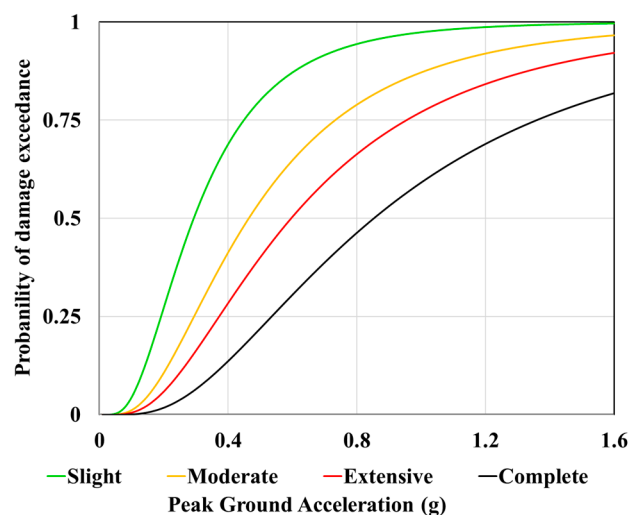


**Figure 2.** Fragility curve for a railway bridge.

For embankment structures, the seismic fragility curves proposed by Argyroudis and Kaynia [16] are the most widely used. In this study, the seismic fragility functions for embankment structures were applied based on subsoil stiffness and embankment height as proposed by Argyroudis and Kaynia [16]. The applied seismic fragility curves vary with the softness of the subsoil. These fragility curves are shown in Table 2 and Figure 3.

**Table 2.** Fragility curve for embankment [16].

(a) Soft ground (H = 6 m)		
Damage State	Median (g)	Standard Deviation ( $\beta$ )
Slight	0.12	0.8
Moderate	0.2	
Extensive	0.34	
(b) Soft ground (H = 4 m)		
Damage State	Median (g)	Standard Deviation ( $\beta$ )
Slight	0.25	0.8
Moderate	0.37	
Extensive	0.54	

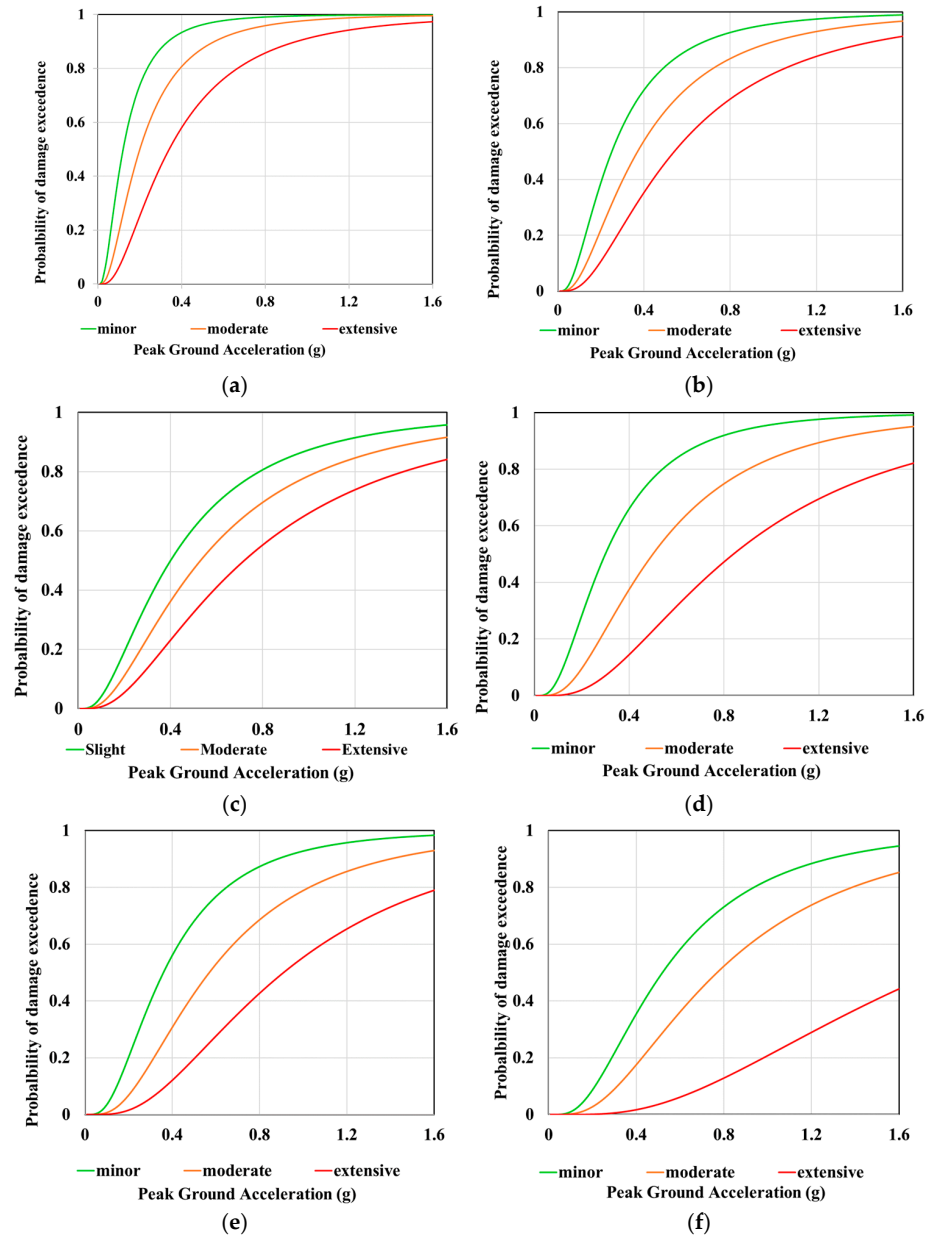
Table 2. Cont.

<b>(c) Soft ground (H = 2 m)</b>		
<b>Damage State</b>	<b>Median (g)</b>	<b>Standard Deviation (<math>\beta</math>)</b>
Slight	0.4	0.8
Moderate	0.53	
Extensive	0.72	
<b>(d) Stiff ground (H = 6 m)</b>		
<b>Damage State</b>	<b>Median (g)</b>	<b>Standard Deviation (<math>\beta</math>)</b>
Slight	0.3	0.7
Moderate	0.5	
Extensive	0.84	
<b>(e) Stiff ground (H = 4 m)</b>		
<b>Damage State</b>	<b>Median (g)</b>	<b>Standard Deviation (<math>\beta</math>)</b>
Slight	0.36	0.7
Moderate	0.57	
Extensive	0.91	
<b>(f) Stiff ground (H = 2 m)</b>		
<b>Damage State</b>	<b>Median (g)</b>	<b>Standard Deviation (<math>\beta</math>)</b>
Slight	0.52	0.7
Moderate	0.77	
Extensive	1.77	

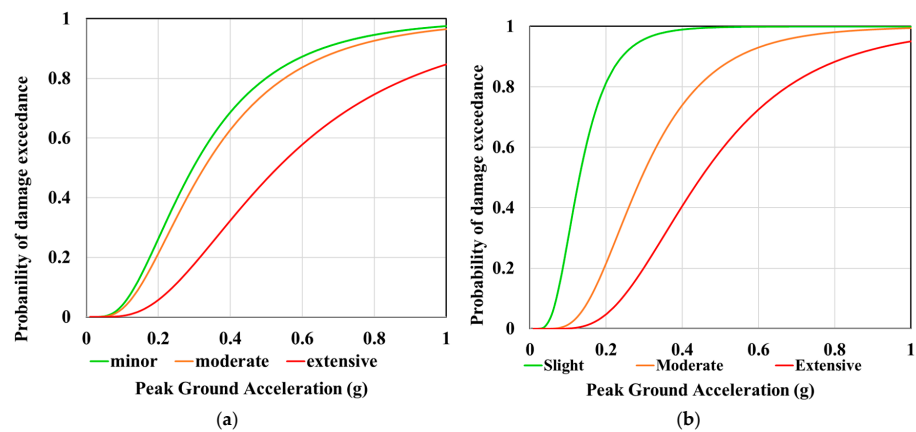
For tunnel structures, seismic fragility curves for cut-and-cover tunnels, which are relatively more vulnerable to earthquakes [17], were applied. Kwon et al. [18] proposed fragility curves for cut-and-cover tunnels by linearly combining four prior models. In this study, the proposed seismic fragility curves were applied to evaluate the seismic resilience of bridge components in the railway network. The fragility curves are shown in Table 3 and Figure 4.

Table 3. Fragility curve for cut-and-cover tunnel [18].

<b>(a) Shallow Tunnel (0–20 m)</b>		
<b>Damage State</b>	<b>Median (g)</b>	<b>Standard Deviation (<math>\beta</math>)</b>
Slight	0.296	0.619
Moderate	0.327	
Extensive	0.531	
<b>(b) Deep Tunnel (Below 20 m)</b>		
<b>Damage State</b>	<b>Median (g)</b>	<b>Standard Deviation (<math>\beta</math>)</b>
Slight	0.13	0.485
Moderate	0.293	
Extensive	0.449	



**Figure 3.** Fragility curve for railway embankment. (a) Soft ground, H = 6 m; (b) soft ground, H = 4 m; (c) soft ground, H = 2 m; (d) stiff ground, H = 6 m; (e) stiff ground, H = 4 m; (f) stiff ground, H = 2 m.



**Figure 4.** Fragility curve for railway tunnel. (a) Shallow tunnel; (b) deep tunnel.

### 2.2.2. Derivation of Restoration Curves for Railway Network Components Based on Damage States

Restoration curves evaluate functionality degradation and recovery times for structures based on their damage states during earthquakes. Restoration models are calculated using the mean and standard deviation of expected recovery times for each damage state of the structures, with Federal Emergency Management Agency [19] values applied for these parameters. Recovery times and standard deviations for bridges, embankments, and tunnels based on damage states are presented in Table 4, and these were used to derive restoration curves. The restoration curves were derived using the mean and standard deviation of recovery times, assuming a normal distribution of recovery times and by calculating probabilities corresponding to specific periods from the cumulative distribution function. The derived restoration curves for railway network components are shown in Figure 5. According to the model, it takes approximately 4 days, 15 days, 261 days, and 716 days for railway bridges to fully recover their functionality after slight, moderate, extensive, and complete damage states, respectively. For embankments, it takes approximately 2 days, 17 days, and 73 days to recover from slight, moderate, and extensive damage states, respectively, while for tunnels, the recovery times are approximately 2 days, 18 days, and 170 days for the respective damage states. The formula for deriving the seismic fragility function is presented in Equation (2).

$$Q[ds|t] = \Phi\left(\frac{\ln Y - \gamma}{\theta}\right) \tag{2}$$

where  $Y$  represents the time required for recovery,  $\gamma$  denotes the median (day), and  $\theta$  represents the standard deviation (days).

**Table 4.** Recovery duration for railway structure [19].

<b>(a) Railway Bridge</b>		
<b>Damage State</b>	<b>Mean (day)</b>	<b>Standard Deviation <math>\sigma</math> (days)</b>
Slight	0.6	0.6
Moderate	2.5	2.7
Extensive	75	42
Complete	230	110
<b>(b) Railway Embankment</b>		
<b>Damage State</b>	<b>Recovery Time (day)</b>	<b>Standard Deviation <math>\sigma</math> (days)</b>
Slight	0.9	0.07
Moderate	3.3	3
Extensive/Complete	40	29
<b>(c) Railway Tunnel</b>		
<b>Damage State</b>	<b>Recovery Time (day)</b>	<b>Standard Deviation <math>\sigma</math> (days)</b>
Slight	0.5	0.3
Moderate	2.4	2
Extensive/Complete	45	30

### 2.2.3. Derivation of Functionality Curves for Railway Network Components Based on Seismic Damage States

To develop functionality loss curves for railway network components based on damage states, functionality curves must first be derived. Functionality curves are derived as expected values by combining the probability of damage occurrence for each damage state and the degree of functionality degradation over time when the damage occurs,

representing the predicted functionality recovery of the structure over time. When there is no functionality loss, the value is 1, while complete functionality loss corresponds to a value of 0. The functionality curves can be calculated using Equation (3).

$$Q(t) = \sum_{i=0}^4 Q[ds_i|t]P[ds_i|IM] \tag{3}$$

where  $Q[ds_i|t]$  represents the functionality level of a structure over time for each damage state,  $P[ds_i|IM]$  represents the probability of each damage state occurring based on earthquake intensity, and  $ds$  represents the damage states. Damage states are categorized into five levels: no damage ( $ds_0$ ), slight damage ( $ds_1$ ), moderate damage ( $ds_2$ ), extensive damage ( $ds_3$ ), and complete collapse ( $ds_4$ ).  $P[ds_i|IM]$  can be calculated using Equations (4)–(6).

$$P[ds_i|IM] = 1 - P[ds > ds_{i+1}|IM], \text{ when } i = 0 \tag{4}$$

$$P[ds_j|IM] = P[ds > ds_j|IM] - P[ds > ds_{j+1}|IM], \text{ when } j = 1, 2, 3 \tag{5}$$

$$P[ds_k|IM] = P[ds > ds_k|IM], \text{ when } k = 4 \tag{6}$$

where  $IM$  represents the intensity of the input earthquake. Through this process, fragility curves and restoration curves can be linearly combined to derive the functionality curve function  $Q(t)$ . The resulting functionality curves for each railway network component are shown in Figure 6.

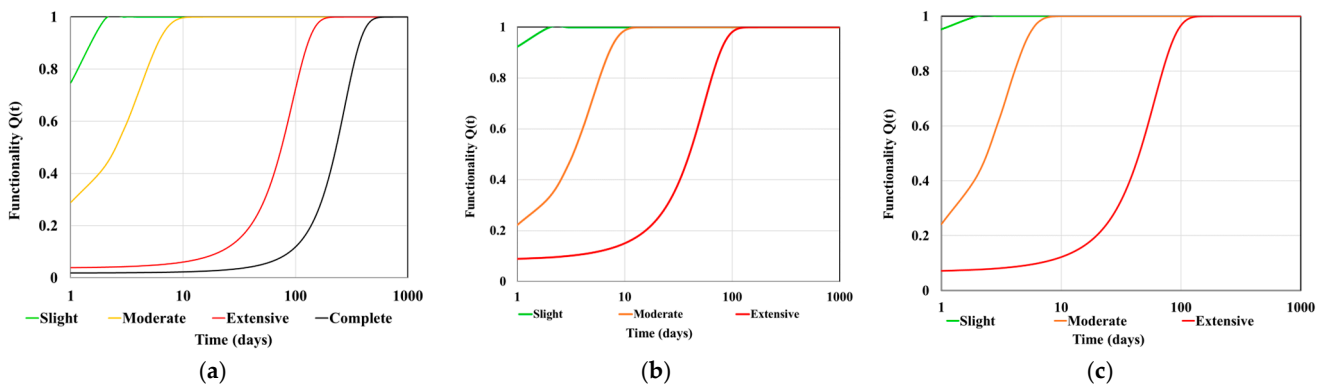


**Figure 5.** Restoration curve for railway embankment and tunnel [19]. (a) Restoration curve for railway bridge; (b) restoration curve for railway embankment; (c) restoration curve for railway tunnel.

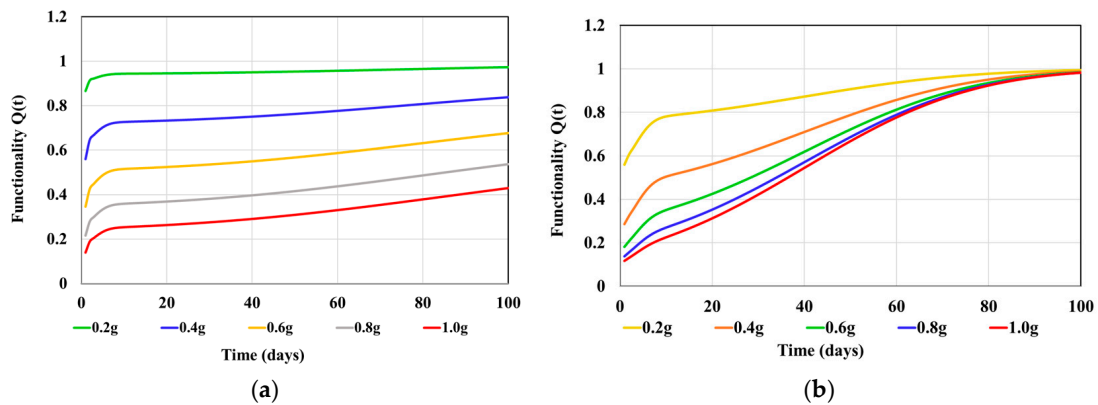


**Figure 6.** Cont.

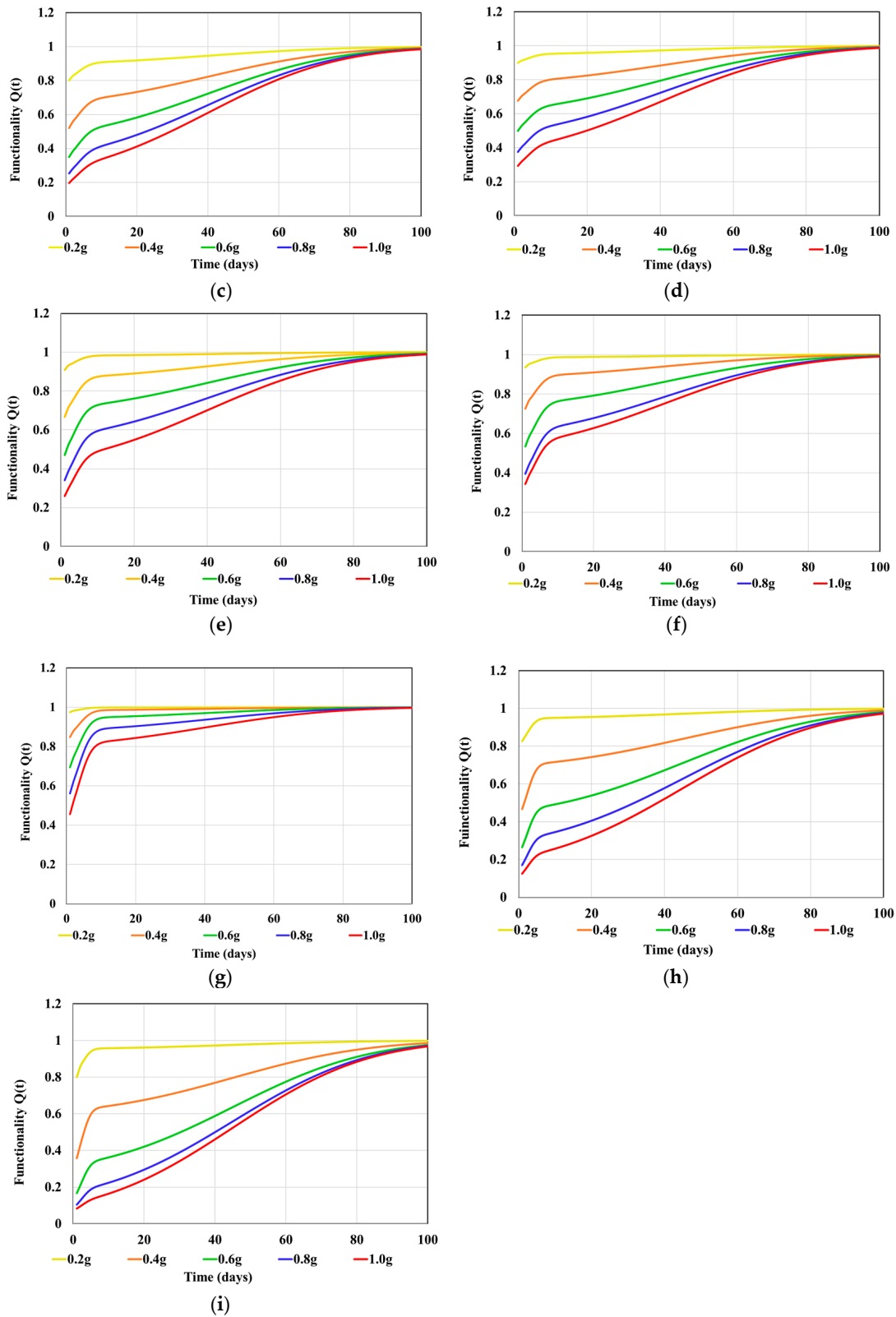


**Figure 6.** Functionality curve for railway structures. (a) Functionality curve for railway bridge; (b) functionality curve for railway embankment on soft ground,  $H = 6$  m; (c) functionality curve for railway embankment on soft ground,  $H = 4$  m; (d) functionality curve for railway embankment on soft ground,  $H = 2$  m; (e) functionality curve for railway embankment on stiff ground,  $H = 6$  m; (f) functionality curve for railway embankment on stiff ground,  $H = 4$  m; (g) functionality curve for railway embankment on stiff ground,  $H = 2$  m; (h) functionality curve for railway shallow tunnel (0–20 m); (i) functionality curve for railway deep tunnel (over 20 m).

### 2.3. Derivation of Functionality Loss Curves for Railway Network Components

To derive functionality loss curves, the evaluation period ( $t_f$ ) for assessing the functionality loss of the railway network must first be defined. The degree of functionality loss for railway structures is calculated as the area of functionality loss compared to a fully functional state, which can vary depending on the evaluation period. As railway structures recover their functionality over time, approaching a value of 1, longer evaluation periods tend to yield functionality loss values closer to 1. Thus, selecting an appropriate evaluation period and deriving functionality loss curves for that period is essential. Once the evaluation period for calculating the functionality loss of railway network components is determined, the extent of functionality loss caused by earthquakes during this period can be quantitatively assessed. In this study, as shown in Figure 7, the evaluation period for functionality loss was set to 100 days. Functionality loss values for railway network components over the 100 days following an earthquake were calculated, as expressed in Equation (7). Here, the 100-day functionality loss evaluation period was determined with reference to the expected recovery times for transportation infrastructure facilities such as railway structures [20].

$$\text{Functionality Loss} = 1 - \frac{\int_{t_0}^{t_f} Q(t)dt}{t_f - t_0} \tag{7}$$

where  $t_f$  is the target time for evaluating functionality loss, and  $t_0$  is the time of the earthquake occurrence.

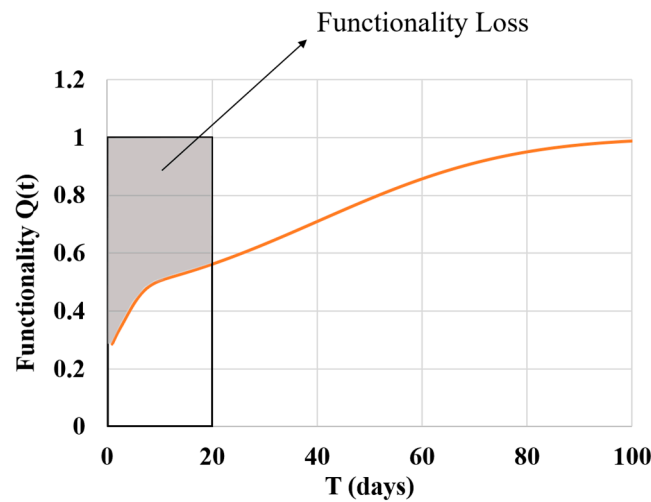


**Figure 7.** Determination of functionality loss for each seismic load (input PGA = 0.4 g; duration = 100 days).

Repeating this process for various input seismic intensities allows functionality loss curves to be derived. The functionality loss curves for each railway network component are shown in Figure 8. Compared to functionality curves, functionality loss curves provide a more intuitive understanding of how much functionality is lost by structures due to seismic intensity. For example, for railway bridge structures, approximately 25% functionality loss occurs at a seismic intensity of 0.4 g, and around 60% functionality loss occurs at 0.8 g. For embankment structures, functionality loss rates tend to increase as embankment height increases. For tunnel structures, relatively higher functionality loss rates were observed in deeper structures.

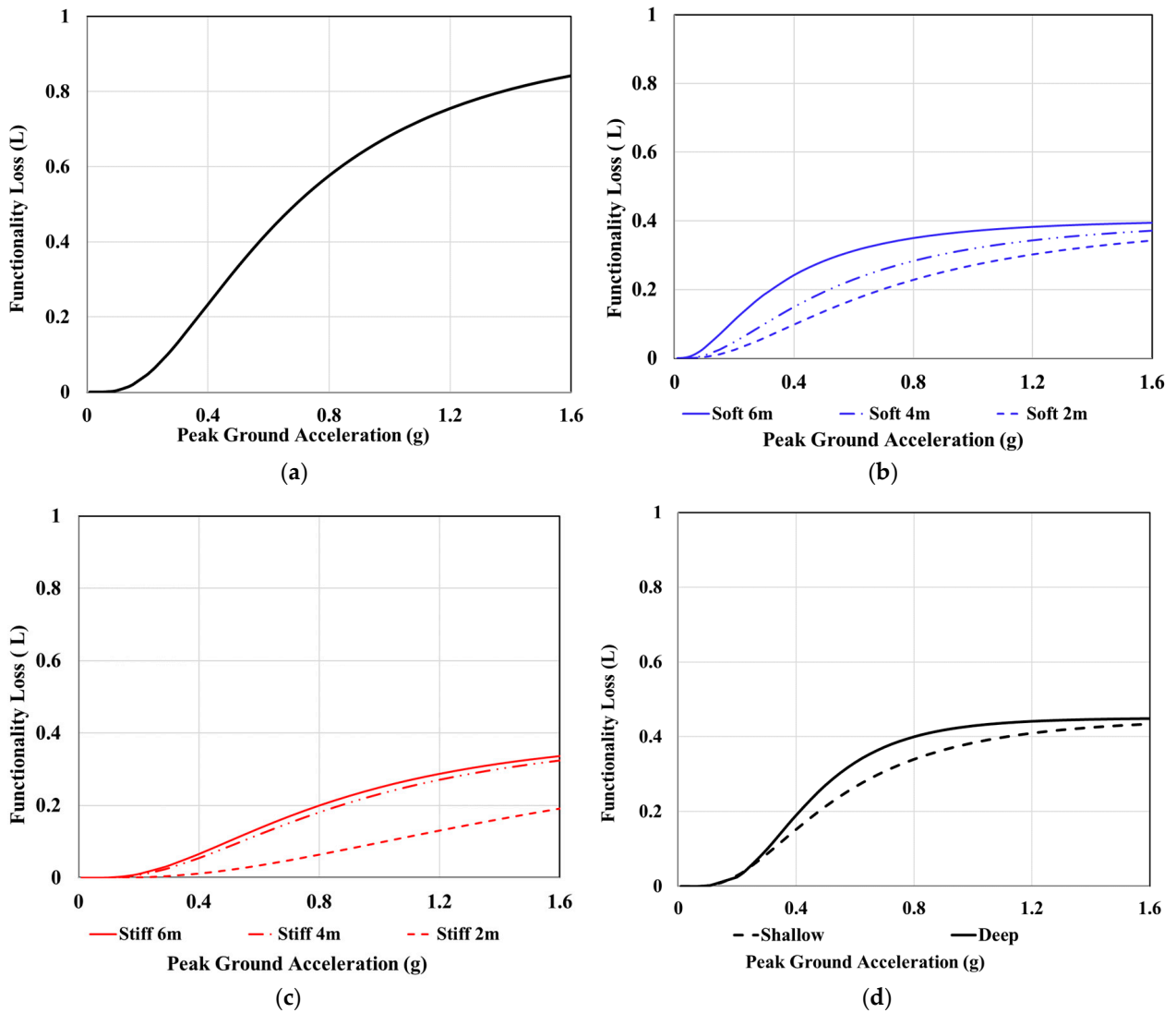


**Figure 8.** Functionality loss curve for railway structures. (a) Functionality loss curve for railway bridge; (b) functionality loss curve for railway embankment (soft ground); (c) functionality loss curve for railway embankment (stiff ground); (d) functionality curve loss for railway tunnel.

*2.4. Annual Occurrence Probability of Functionality Loss for the Railway Network System*

The annual occurrence probability of functionality loss was derived using the seismic intensities for return periods and degrees of functionality loss specified in the seismic design standards of Korea [21]. For the annual exceedance probability, the earthquake magnitude that could occur annually was calculated using the inverse of the return period specified in the seismic design standards of Korea. Based on this calculation, the functionality loss values were determined. Since ground amplification varies depending on the type of ground, all ground conditions were uniformly assumed to be S1, representing a rock condition with no amplification. It was used to estimate the annual probability of functionality loss for each railway network component in the railway network. The results are shown in Figure 9.

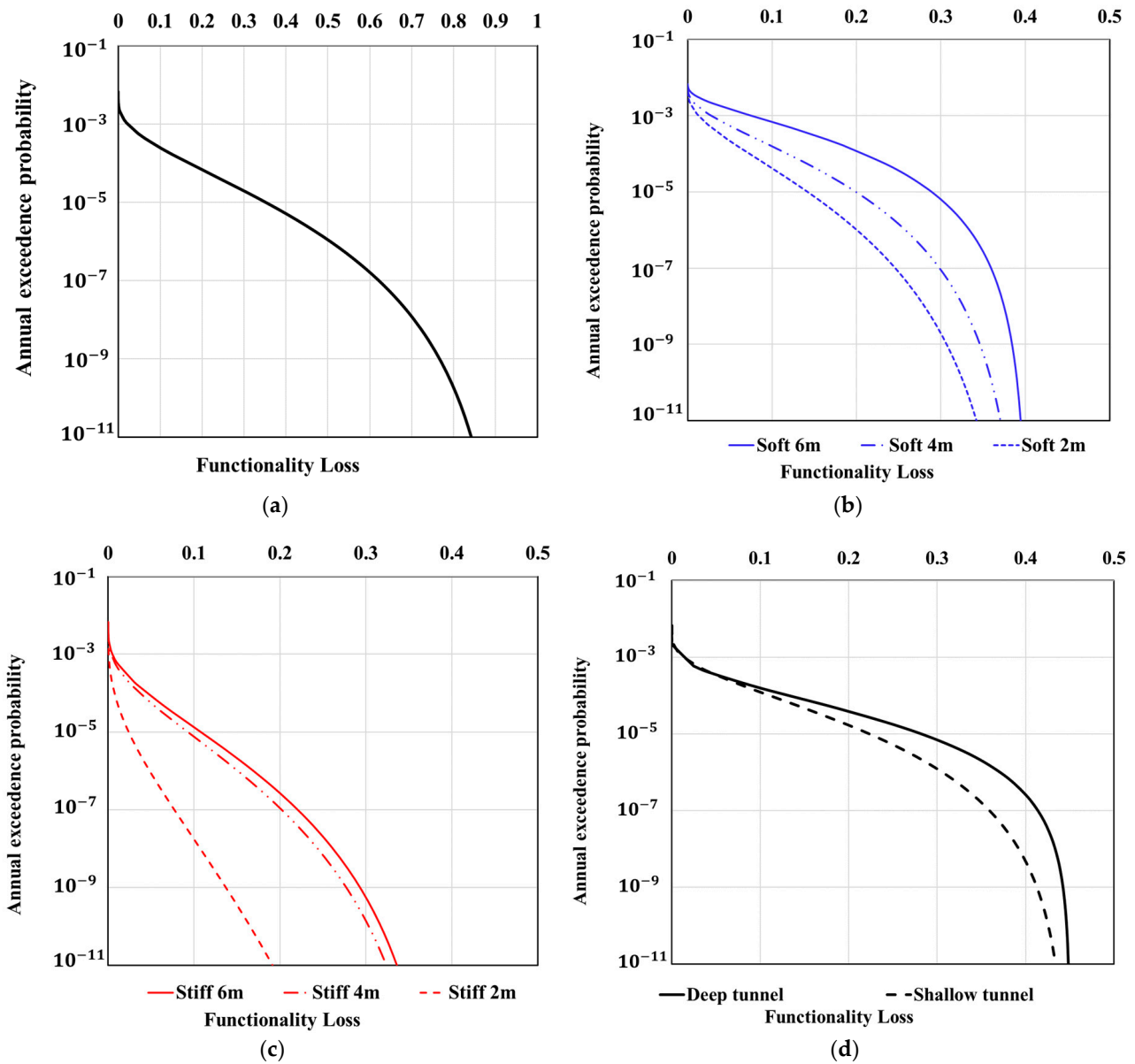


**Figure 9.** Annual exceedance probability for railway structures. (a) Annual exceedance probability for railway bridge; (b) annual exceedance probability for railway embankment (Soft ground); (c) annual exceedance probability for railway embankment (stiff ground); (d) annual exceedance probability for railway tunnel.

### 3. Application of Functionality Loss Evaluation Model for Railway Network Components

#### 3.1. Construction and Visualization of the Railway Network Model

To assess the applicability of the functionality loss evaluation model for railway network components, a hypothetical railway network system was constructed. The hypothetical railway network system was assumed to be a branching system rather than a single line, referencing various railway systems in Korea and abroad. The proposed network system for evaluation was designed with three lines, allowing different routes to remain operational depending on the damaged sections, thereby increasing the diversity of network impact scenarios based on functionality loss. Line 1 spans 29 km and includes 10 railway components (three railway bridges, four embankment sections, and three tunnels); Line 2 spans 11 km and includes four railway components (one railway bridge, two embankment

sections, and one tunnel); and Line 3 spans 15 km and includes six railway components (one railway bridge, four embankment sections, and one tunnel). To define fragility functions for embankment and tunnel sections, parameters such as embankment height, subsoil stiffness, and tunnel depth were assumed to ensure diversity in functionality loss levels. The assumed input conditions are shown in Table 5.

Table 5. Structure condition for embankment and tunnel.

	Height (Embankment)/Depth (Tunnel)	Ground Stiffness
Embankment 1	2	Stiff ground
Embankment 2	4	Soft ground
Embankment 3	6	Stiff ground
Embankment 4	2	Soft ground
Embankment 5	4	Stiff ground
Embankment 6	6	Soft ground
Embankment 7	2	Stiff ground
Embankment 8	4	Soft ground
Embankment 9	6	Stiff ground
Embankment 10	4	Soft ground
Tunnel 1	shallow	
Tunnel 2	deep	
Tunnel 3	shallow	
Tunnel 4	deep	
Tunnel 5	deep	

The hypothetical railway network proposed in this study for applying the functionality loss evaluation model for railway network components is visualized in Figure 10. Additionally, although actual railway networks are much more diverse and complex than the railway network proposed in this study, a simplified design was adopted to facilitate a more convenient evaluation of the functionality assessment process for structures. Railway bridge sections are displayed in gray, while tunnel sections are displayed in black. Additionally, embankment sections on soft ground are marked in light yellow, and those on stiff ground are marked in orange.

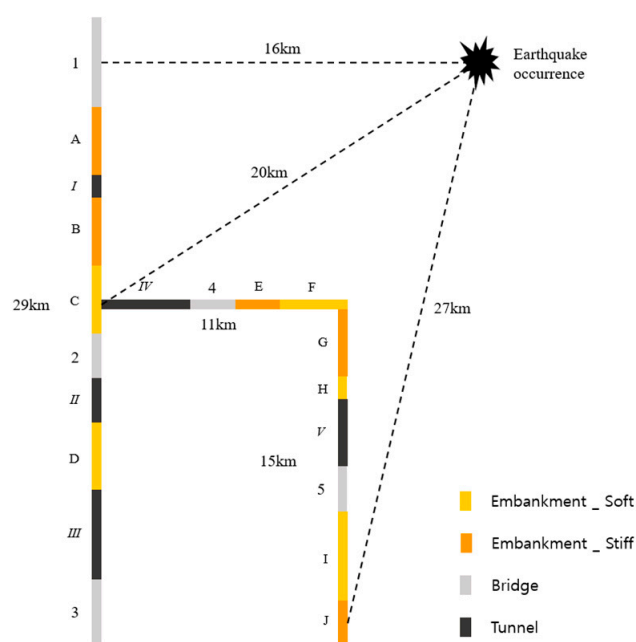


Figure 10. Seismic resilience value for an earthquake scenario.

### 3.2. Application of Functionality Loss Evaluation Model for Structures Under Earthquake Scenarios: Case 1

#### 3.2.1. Earthquake Scenario: 0.3 g

To take a more conservative approach, this study assumed an earthquake scenario with a seismic acceleration of 0.3 g, which exceeds the maximum seismic acceleration (0.286 g) specified in the seismic design standard KDS 17 10 00 of Korea [21]. The earthquake was assumed to occur at a location 16 km from the railway lines, with all railway network components located within 32 km of the epicenter. The earthquake depth was assumed to be a shallow 10 km, similar to the Pohang earthquake that occurred in Korea. Based on this scenario, the distances from the epicenter to each railway facility were used to calculate the rock seismic acceleration affecting the railway structures. The maximum rock acceleration at the epicenter was assumed to be 0.3 g, and the maximum rock acceleration values at the location of each structure were calculated to decrease proportionally with distance. When an earthquake occurs at the hypocenter, seismic waves propagate along the bedrock, causing the rock acceleration to decrease with distance from the epicenter due to damping. Subsequently, as the seismic waves propagate near the surface, they are amplified due to the site response. The characteristics of the site response are determined by the shear velocity of the soil within 30 m below the surface and the depth of the bedrock. To incorporate the amplification of seismic acceleration due to local site response, the ground conditions at the locations of each component were assumed based on the ground classification in KDS 17 10 00 [21], as shown in Table 6. For embankments, the subsoil stiffness was assumed as specified in Table 7. The ground amplification factors ( $F_a$ ) from Table 7 of KDS 17 10 00 [21] were then applied to each railway network component to calculate the final peak ground acceleration (PGA).

**Table 6.** Ground condition for each railway network structure.

Structure	Soil Classification	Structure	Soil Classification
Bridge 1	S2	Embankment A	S2
Bridge 2	S3	Embankment B	S4
Bridge 3	S4	Embankment C	S3
Bridge 4	S4	Embankment D	S5
Bridge 5	S5	Embankment E	S2
Tunnel 1	S3	Embankment F	S3
Tunnel 2	S3	Embankment G	S4
Tunnel 3	S2	Embankment H	S5
Tunnel 4	S3	Embankment I	S3
Tunnel 5	S2	Embankment J	S4

**Table 7.** Short-period amplification factors [21].

Ground Type	Description	Short-Period Ground Amplification Factor, $F_a$		
		$S \leq 0.1$	$S = 0.2$	$S \geq 0.3$
S <sub>2</sub>	Shallow and stiff ground	1.4	1.4	1.3
S <sub>3</sub>	Shallow and soft ground	1.7	1.5	1.3
S <sub>4</sub>	Deep and stiff ground	1.6	1.4	1.2
S <sub>5</sub>	Deep and soft ground	1.8	1.3	1.3

#### 3.2.2. Derivation of Functionality Loss for Railway Network Components Under an Earthquake Scenario

The calculated PGA and functionality loss values for each railway network component are presented in Figure 11 and Table 8. Functionality losses of <2%, >2%, >4%, and >10% are

shown in yellow, green, orange, and red, respectively, to illustrate the extent of functionality loss. Overall, functionality loss occurred mainly in embankment sections on soft ground, while railway bridges exhibited the lowest functionality loss. The estimated functionality loss ranged from 1.8 to 6.7% for railway bridge sections, 2.4–17.2% for embankment sections on soft ground, 0.2–1.3% for embankment sections on stiff ground, and 1.0–4.6% for tunnel sections. However, this study applied the same seismic fragility function for bridges and classified tunnels only by depth, applying the same seismic fragility function for each category, which presents a limitation. Additionally, since a wide range of sections were not simulated, similar peak ground acceleration values were derived despite considering ground amplification, leading to similar functionality loss values for the same structures. The objective of this study is to propose and apply a methodology for determining functionality loss in railway networks based on previous studies. It is anticipated that establishing a classification system for structures based on various parameters and deriving seismic fragility functions for each classification will lead to more reasonable results in the future.

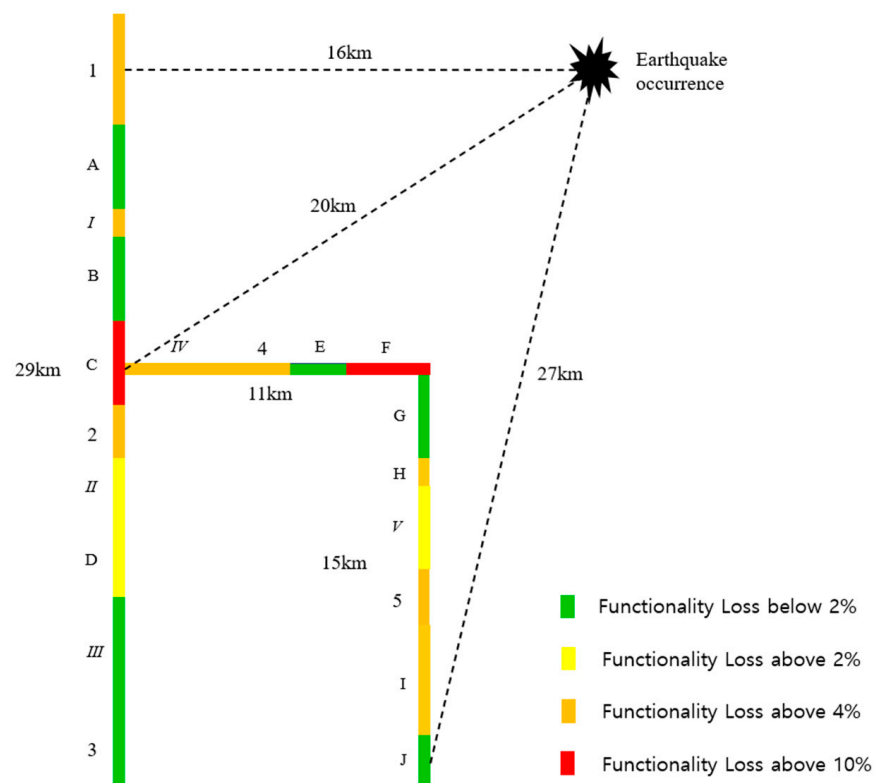


Figure 11. Functionality loss value for earthquake scenario (Input PGA = 0.3 g).

Table 8. Calculated PGA value and functionality loss value at each structure (input PGA = 0.3 g).

Label	Length (m)	Distance from Epicenter (km)	PGA Level (g)	Functionality Loss (%)
Bridge No. 1	4	16	0.22260	6.28
Bridge No. 2	2	22	0.20505	5.00
Bridge No. 3	3	31	0.14736	1.78
Bridge No. 4	2	17	0.22752	6.66
Bridge No. 5	2	20	0.21858	5.98
Embankment A	3	17	0.22263	0.18
Embankment B	3	19	0.21246	0.96
Embankment C	4	20	0.21891	12.58
Embankment D	3	24	0.19882	2.36

Table 8. Cont.

Label	Length (m)	Distance from Epicenter (km)	PGA Level (g)	Functionality Loss (%)
Embankment E	2	15	0.23297	1.29
Embankment F	3	13	0.28062	17.21
Embankment G	3	15	0.24415	0.25
Embankment H	1	16	0.23929	6.69
Embankment I	4	23	0.19866	4.64
Embankment J	2	27	0.16584	0.57
Tunnel I	1	18	0.23436	4.62
Tunnel II	2	23	0.19866	2.46
Tunnel III	4	27	0.14587	0.99
Tunnel IV	4	19	0.22643	4.04
Tunnel V	3	18	0.20397	2.73

### 3.2.3. Derivation of Functionality Loss for the Railway Network System Under an Earthquake Scenario 0.3 g

To evaluate the overall functionality loss of the railway network, two methods can be used: (1) using the maximum loss value or (2) calculating the average functionality loss of all network components using Equation (8).

$$FL_N = \frac{L_S \times FL_S}{L_N} \quad (8)$$

where  $FL_N$  is the railway network functionality loss ratio,  $FL_S$  is the functionality loss ratio of railway components, and  $L$  is the length of the component.

Assuming that functionality loss in any single section causes an overall functionality loss for the entire network, the functionality loss ratios for Line 1 (12.58% at embankment section C), Line 2 (17.21% at embankment section F), and Line 3 (6.69% at embankment section H) can be evaluated. Notably, embankment section C has the greatest impact on the functionality of the entire network, as its functionality loss disrupts the connections between Line 1 and Lines 2 and 3. Thus, its functionality loss value of 12.58% can be considered the representative value for network functionality loss. If this evaluation method is considered to overestimate functionality loss, calculations using Equation (6) yield a railway network functionality loss ratio of 3.99%.

## 3.3. Application of the Functionality Loss Evaluation Model for Structures Under Earthquake Scenarios: Case 2

### 3.3.1. Earthquake Scenario: 0.5 g

While the earlier scenario assumed a seismic acceleration of 0.3 g based on the seismic design standards of Korea, an additional analysis was conducted using a more extreme earthquake scenario with a seismic acceleration of 0.5 g.

### 3.3.2. Derivation of Functionality Loss for Railway Network Components Under the Earthquake Scenario

The calculated PGA and functionality loss values for each railway network component are presented in Figure 12 and Table 9. Functionality loss values of <5%, >5%, >15%, and >20% are represented in yellow, green, orange, and red, respectively, to illustrate the extent of functionality loss. Overall, functionality loss occurred mainly in embankment sections on soft ground, while railway bridges exhibited the lowest functionality loss. The estimated functionality loss ranged from 6.9 to 18.9% for railway bridge sections, 4.3–24.0% for embankment sections on soft ground, 0.8–4.5% for embankment sections on stiff ground, and 5.1–12.9% for tunnel sections.

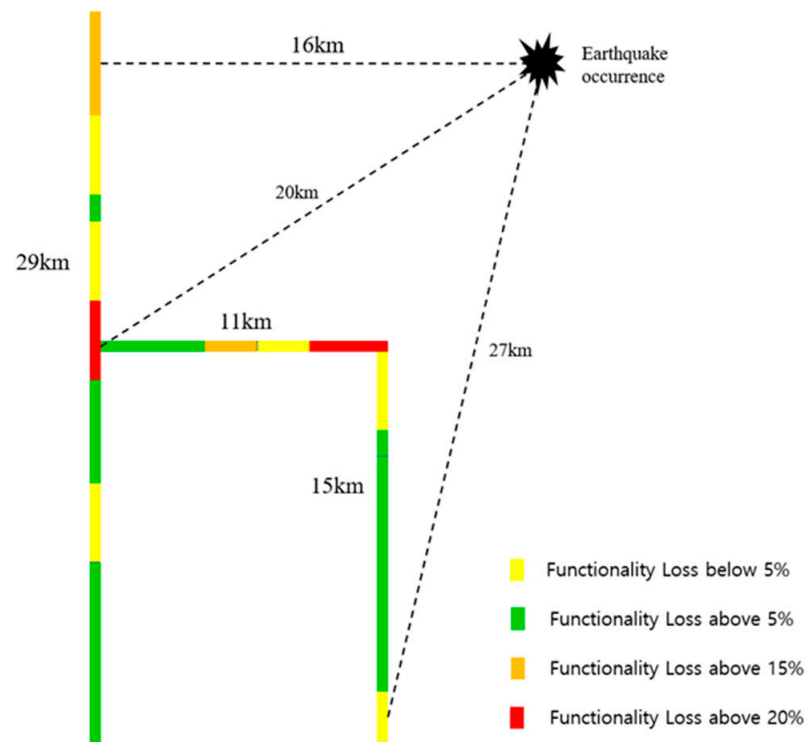


Figure 12. Functionality loss value for earthquake scenario (input PGA = 0.5 g).

Table 9. Calculated PGA value and functionality loss value at for structure (input PGA = 0.5 g).

Label	Length (m)	Distance from Epicenter (km)	PGA Level (g)	Functionality Loss (%)
Bridge No. 1	4	16	0.35377	18.85
Bridge No. 2	2	22	0.30750	14.07
Bridge No. 3	3	31	0.22918	6.89
Bridge No. 4	2	17	0.32778	16.14
Bridge No. 5	2	20	0.29069	12.41
Embankment A	3	17	0.35377	0.82
Embankment B	3	19	0.31071	2.94
Embankment C	4	20	0.32485	20.10
Embankment D	3	24	0.25740	4.28
Embankment E	2	15	0.36684	4.47
Embankment F	3	13	0.39631	24.01
Embankment G	3	15	0.34538	0.77
Embankment H	1	16	0.34450	12.18
Embankment I	4	23	0.29930	9.84
Embankment J	2	27	0.25227	2.13
Tunnel I	1	18	0.34344	11.45
Tunnel II	2	23	0.29930	9.75
Tunnel III	4	27	0.24312	5.10
Tunnel IV	4	19	0.33400	12.92
Tunnel V	3	18	0.32955	12.50

### 3.3.3. Derivation of Functionality Loss for the Railway Network System Under an Earthquake Scenario 0.5 g

To evaluate the overall functionality loss of the railway network, two methods can be used: (1) using the maximum loss value or (2) calculating the average functionality loss of all network components using Equation (9).

$$FL_{network} = \frac{L_{structure} * FL_{structure}}{L_{network}} \quad (9)$$

where  $FL$  is the functionality loss ratio, and  $L$  is the length of the component.

The functionality loss for the railway network, calculated using the same method as before, is as follows: Assuming that functionality loss in any single section causes an overall functionality loss for the entire network, the functionality loss ratios for Line 1 (20.1% at embankment section C), Line 2 (24% at embankment section F), and Line 3 (12.2% at embankment section H) can be evaluated. Notably, embankment section C has the greatest impact on the functionality of the entire network, as its functionality loss disrupts the connections between Line 1 and Lines 2 and 3. Thus, its functionality loss value of 20.1% can be considered the representative value for network functionality loss. If this evaluation method is considered to overestimate functionality loss, calculations using Equation (9) yield a railway network functionality loss ratio of 9.57%. To quantitatively evaluate the socioeconomic impact of earthquakes, such as disruptions in logistics, caused by functionality loss in railway networks, it is essential to accurately calculate the functionality loss ratio. While this study proposes a preliminary method based on functionality loss of components, future research on the spatial correlation of structural damage caused by earthquakes is expected to enable more precise evaluations of the impact of component functionality loss on overall network functionality and socioeconomic losses.

#### 4. Conclusions

This study proposed a model to evaluate functionality loss during earthquakes that uses existing seismic fragility curves and statistical recovery time data for railway network components, including bridges, embankments, and tunnels. The proposed model was applied to a hypothetical railway network system to estimate the functionality loss in actual railway infrastructure during extreme earthquake scenarios.

1. Functionality loss evaluation models were derived for railway network components, including bridges, tunnels, and embankment sections. To develop functionality loss evaluation models for railway network components, seismic fragility curves for each component were analyzed, and restoration curves were derived using statistical recovery time data. Procedures for deriving functionality curves and functionality loss curves by combining seismic fragility curves and restoration curves were outlined.
2. The developed evaluation model for functionality loss of railway network components during earthquakes was applied to the Comprehensive Railway Test Line in Korea, and its applicability was assessed. To assume extreme earthquake scenarios, seismic scenarios with a seismic acceleration of 0.3 g, which exceeds the maximum 0.286 g specified in the seismic design standards of Korea, and an extreme scenario with 0.5 g were used. The distance of components was set within 32 km from the epicenter, and the depth was assumed to be shallow (10 km), similar to the Pohang earthquake.
3. For a 0.3 g earthquake, the estimated functionality loss for railway network components was 1.8–6.7% for bridge sections, 2.4–17.2% for embankments on soft ground, 0.2–1.3% for embankments on stiff ground, and 1.0–4.6% for tunnel sections. Two methods can be used to evaluate the functionality loss of the entire railway network: (1) using the maximum value or (2) calculating the average functionality loss of all network components. Using the first method, the functionality loss values for Lines 1, 2, and 3 were 12.58%, 17.21%, and 6.69%, respectively. Particularly, embankment section C had the greatest impact on the overall network, with its functionality loss of 12.58% being considered the representative functionality loss value. Using the second method, the average functionality loss ratio for the network was 3.99%.

4. For the extreme 0.5 g earthquake scenario, the representative functionality loss value was 20.1% using the same method, and the average functionality loss ratio was 9.57%. The series of analysis indicates that the functionality loss of a specific section can lead to disruptions in the overall logistics functionality of the railway network. Further studies should analyze the impact of the functionality loss of specific components on the entire network and conduct research to evaluate functionality loss at the network level. Based on this study, the functionality loss of railway network components during earthquakes, as well as the overall functionality loss of the railway network, can be quantitatively evaluated. This serves as a critical indicator for quantitatively assessing the socioeconomic impact such as disruptions in logistics caused by earthquakes.
5. This study focuses on proposing a methodology for evaluating the functionality loss of railway networks under various earthquake magnitudes. However, the case study applied in this research has two limitations. First, the scope of the railway network was not extensive, resulting in similar peak ground accelerations affecting most structures, and identical seismic fragility functions were applied uniformly within each component classification, leading to nearly identical functionality loss values for bridges, embankments, and tunnels. Second, the spatial correlation of seismic wave propagation and structural damage was not sufficiently considered, resulting in a lack of in-depth analysis of the socioeconomic impacts.
6. To address these limitations, first, future research should establish a rational classification system for railway network components and derive seismic fragility curves for each classification, enabling a more reasonable evaluation of functionality loss for individual components using the proposed model. Second, analyzing the spatial correlation of regions where each railway network component is located during an earthquake and the spatial correlation of how damage to each component affects overall logistics would allow for the design of a more diverse and complex railway network that resembles real-world scenarios. By integrating the spatial correlation of damage into the analysis, it will be possible to evaluate detailed logistics disruptions and provide a more precise assessment of socioeconomic losses. Third, validating the model using actual data on socioeconomic impacts from earthquake-induced damage would enhance its practical applicability. Finally, it is anticipated that future studies could identify safe thresholds for functionality loss requiring system shutdown, enabling the proposal of a safe shutdown earthquake threshold.

**Author Contributions:** M.Y.: Writing—original draft preparation, methodology. J.J.: conceptualization, visualization. S.H.: Writing—methodology, review and editing, visualization. S.K.: Writing—review and editing, supervision, project administration. All authors have read and agreed to the published version of the manuscript.

**Funding:** This research was supported by the Korea Agency for Infrastructure Technology Advancement (KAIA) grant funded by the Ministry of Land, Infrastructure and Transport (Grant No. RS-2023-00238458) and the internal grant (code: 20240366-001, Project Name: Basic research on the development of dynamic complex behavior analysis method and risk management technology for engineered barrier system for deep disposal of high-level radioactive waste) from the Korea Institute of Civil Engineering and Building Technology (KICT), Republic of Korea. We appreciate the support provided.

**Data Availability Statement:** Data are contained within the article.

**Conflicts of Interest:** The authors declare no conflicts of interest.

## Notion

$P[ds_i IM]$	the probability of exceedance for each damage state based on seismic intensity
$X$	peak ground acceleration
$\mu$	median of peak ground acceleration (g)
$\beta$	standard deviation of peak ground acceleration
$Q[ds_i t]$	the functionality over time for each damage state
$\gamma$	median of recovery time (day)
$\theta$	standard deviation of recovery time
$Q(t)$	functionality of structure
$t_f$	evaluation period
$t_0$	time of the earthquake occurrence
$FL_N$	the railway network functionality loss ratio
$FL_S$	the functionality loss ratio of railway components

## References

- Hemeda, S. Geotechnical modelling and subsurface analysis of complex underground structures using PLAXIS 3D. *Int. J. Geo Eng.* **2022**, *13*, 9. [CrossRef]
- Argyroudis, S.A.; Pitilakis, K.D. Seismic fragility curves of shallow tunnels in alluvial deposits. *Soil Dyn. Earthq. Eng.* **2012**, *35*, 1–12. [CrossRef]
- Jin, H.S.; Song, J.K. Effect of near- and far-fault earthquakes for seismic fragility curves of PSC box girder bridges. *J. Earthq. Eng. Soc. Korea* **2010**, *14*, 53–64. [CrossRef]
- Kyung, J.B.; Kim, M.J.; Lee, S.J.; Kim, J.K. An analysis of probabilistic seismic hazard in the Korean Peninsula. *J. Korean Earth Sci. Soc.* **2016**, *37*, 52–61. [CrossRef]
- Nguyen, A.-D.; Nguyen, V.-T.; Kim, Y.S. Finite element analysis on dynamic behavior of sheet pile quay wall dredged and improved seaside subsoil using cement deep mixing. *Int. J. Geo Eng.* **2023**, *23*, 9. [CrossRef]
- Yoo, M.; Kwon, S.Y.; Hong, S. Dynamic response evaluation of deep underground structures based on numerical simulation. *Geomech. Eng.* **2022**, *29*, 269–279.
- Kim, M.G.; Hong, S.G.; Park, S.H.; Kim, Y.S.; Kim, H.G. A Study on the Localization of Seismic Fragility Functions for Railway Facilities. Research Report by the Korea Agency for Infrastructure Technology Advancement, 2008. Available online: <https://dl.nanet.go.kr/> (accessed on 25 September 2024).
- Lee, Y.S. Seismic performance evaluation and development of seismic fragility functions for tunnels on the Gyeongbu high-speed railway. *J. Korean Earthq. Eng. Soc.* **2014**, *15*, 67–75. [CrossRef]
- Yang, S.H.; Kwak, D.Y. Development of seismic fragility curves for high-speed railway systems. *J. Korean Geotech. Soc.* **2019**, *23*, 123–132.
- Avanaki, M.J.; El Naggar, H.; El Naggar, S. Seismic fragility assessment of fibre-reinforced concrete segmental tunnel linings. *Tunn. Undergr. Space Technol.* **2018**, *81*, 32–46.
- Andreotti, G.; Lai, C.G. Seismic vulnerability assessment of mountain tunnels using fragility curves. *Bull. Earthq. Eng.* **2019**, *17*, 6323–6345.
- Hu, X.; Zhou, Z.; Chen, H.; Ren, Y. Seismic fragility analysis of tunnels with different buried depths in a soft soil. *Sustainability* **2020**, *12*, 892. [CrossRef]
- Kim, J.H.; Kim, H.; Yoo, M.; Ha, I.S. Research on development and application of earthquake risk assessment model for railway structures. *J. Korean Soc. Railw.* **2023**, *26*, 652–663. [CrossRef]
- Huang, Z.; Zhang, D.; Pitilakis, K.; Tsinidis, G.; Huang, H.; Zhang, D.; Argyroudis, S. Resilience assessment of tunnels: Framework and application for tunnels in alluvial deposits exposed to seismic hazard. *Soil Dyn. Earthq. Eng.* **2022**, *162*, 107456. [CrossRef]
- Yang, S.; Kwak, D. Evaluation of seismic fragility models for cut-and-cover railway tunnels. *J. Korean Tunn. Undergr. Space Assoc.* **2021**, *24*, 1–13.
- Argyroudis, S.; Kaynia, A.M. Analytical seismic fragility functions for highway and railway embankments and cuts. *Earthq. Engng. Struct. Dyn.* **2015**, *44*, 1863–1879. [CrossRef]
- Park, S.Y.; Yoon, H.J.; Oh, Y.S.; Sin, Y.S. A case study of damages on tunnel structure due to chuetsu earthquake. In *Proceedings of the KSR (Korean Society for Railway) Conference*; The Korean Society for Railway: Daejeon, Republic of Korea, 2006; pp. 478–492.
- Kwon, S.Y.; Kim, J.; Kwak, D.; Yang, S.; Yoo, M. Development of seismic fragility function for underground railway station structures in Korea. *Buildings* **2024**, *14*, 1200. [CrossRef]
- Federal Emergency Management Agency. *HAZUS-MH Technical Manual*; Federal Emergency Management Agency: Washington, DC, USA, 2024; pp. 7–26.

20. Zhan, S.; Chang-Richards, A.; Elwood, K.; Boston, M. Post-earthquake functional recovery: A critical review. In Proceedings of the 2022 New Zealand Society for Earthquake Engineering Annual Technical Conference, Wellington, New Zealand, 27–29 April 2022; New Zealand Society for Earthquake Engineering: Wellington, New Zealand, 2022.
21. Ministry of Land, Infrastructure and Transportation. *Korean Design 00: Seismic Design Standard*; Ministry of Land, Infrastructure and Transportation: Sejong, Republic of Korea, 2019; Volume 10.

**Disclaimer/Publisher’s Note:** The statements, opinions and data contained in all publications are solely those of the individual author(s) and contributor(s) and not of MDPI and/or the editor(s). MDPI and/or the editor(s) disclaim responsibility for any injury to people or property resulting from any ideas, methods, instructions or products referred to in the content.